We are IntechOpen, the world's leading publisher of Open Access books Built by scientists, for scientists

6,900
Open access books available

186,000
International authors and editors

200M
Downloads

154
Countries delivered to

Our authors are among the

TOP 1%
most cited scientists

12.2%
Contributors from top 500 universities

CLARIVATE ANALYTICS
BOOK CITATION INDEX
INDEXED

WEB OF SCIENCE™

Selection of our books indexed in the Book Citation Index
in Web of Science™ Core Collection (BKCI)

Interested in publishing with us?
Contact book.department@intechopen.com

Numbers displayed above are based on latest data collected.
For more information visit www.intechopen.com

Dual Port Ultra Wideband Antennas for Cognitive Radio and Diversity Applications

Gijo Augustin , Bybi P. Chacko and Tayeb A. Denidni

1. Introduction

Ultra-wideband (UWB) technology has become one of the most promising technology for short- range high speed data communication due to its high data transmission rate and large bandwidth. These systems utilize the frequency band from 3.1GHz to 10.6 GHz, which is allocated to the UWB systems by the Federal Communications Commission (FCC) [1]. In this ultra-wide spectrum, several unlicensed short range communication bands are overlapping such as IEEE 802.11a WLAN and HIPERLAN/2. Therefore, one of the most effective technique to eliminate these intereferences is to integrate a narro band reject filter in the UWB antenna [2-4].

In this emerging technology, antenna plays the role of a key system element. The design of low profile, easy to construct antennas in a limited space with good radiation characteristics is a challenging task for antenna engineers. The planar antennas are very attractive mainly because of their interesting physical features such as simple structure, compactness and low manufacturing cost [5, 6]. However, the requirements such as via-hole connection in probe-fed antennas, larger ground plane size in microstrip fed designs and precise alignment between layers in multilayer configurations result in increased system complexity. One of the most commonly used feeding technique for modern antennas is the Coplanar Waveguide(CPW) which facilitates key advantages such as low dispersion, less radiation loss and ease of integration with monolithic microwave integrated circuits in uniplanar configuration [7].

In this chapter, we present a comprehensive study on the design, analysis, and characterization of two Uniplanar Ultra Wide-Band(UWB) antennas which have the potential to serve the requirements of future wireless communication systems. The studies were also extended to pulse based, time domain analysis to ensure that it will enable rich broadband services of data, voice, HD video along with high speed internet.

In the first section of the chapter, we present an integrated uniplanar UWB antenna for category A cognitive radio application. The Federal Communications Commission (FCC) defines a cognitive radio as "a radio that can change its transmitter parameters based on the interaction with the environment in which it operates" [8]. This concept has originated from the urgent need to effectively utilize the available spectrum with the explosive growth in high-data rate wireless services. In general, cognitive radio networks can utilize different spectrum sensing and allocation methods namely category A and category B, in which category A uses two antennas. In these systems one antenna is wideband, feeding a receiver for spectrum sensing task meanwhile, the second antenna feeds a front end that can be tuned to the selected transmission band. The motivation behind this work is to illustrate a new integrated antenna for category A cognitive-radio systems by utilizing the uniplanar properties of coplanar wave guide [7], time domain characteristics of vivaldi inspired antennas [9] and recent developments in antenna integration techniques [10]. Although cognitive radio may initially cover lower frequencies, the integration method is demonstrated through UWB and WLAN bands.

A uniplanar antenna for diversity application is presented in the second section of this chapter. Diversity techniques are highly desirable in modern wireless communication systems to increase the channel capacity and to combat the multipath fading problem in the environment, which usually causes larger degradation in the system performance [11, 12]. There are different types of diversities and they are categorized in a broad perspective as spatial diversity, pattern diversity and polarization diversity [13-15]. Depending on the environment, footprint specificatons and the expected interference, designers can employ one or more of these methods to achieve diversity gain. In this era of compact wireless communication systems, the pattern or polarization diversity is more suitable for portable devices than spatial diversity. In present wireless communication systems, particularly in a dense environment, a UWB system with diversity technique is a promising solution to enhance the system performance with high data rate and improved resolution [13, 16]. Such a system has potential applications in advanced instruments for microwave imaging, weapon detection radar which uses short impulses and require high speed data transfer. There have been significant efforts in recent years in various designs of dual polarized UWB antennas for future wireless communication systems [14, 17-21]. However most of them offers a large size [17] multilayer structure [14, 18], complex feeding network [20] and not equipped with band notch functionality [19].To full fill this gap, a compact, uniplanar, CPW fed, dual polarized UWB antenna with embeded notch filter is presented in this chapter.

2. Integrated wide-narrowband antenna for cognitive radio applications

2.1. Antenna geometry and design

Geometry: The evolution of integrated wide-narrowband antenna configuration along with associated parameters is shown in Figure1. The antenna lies in the XZ-plane with its normal direction being parallel to the Y-axis. Compared to the existing integrated antennas for cog-

nitive radio application [10, 22, 23] this design has advantages of uniplanar configuration, group delay variation less than 1ns and good isolation between the ports. The major design elements of this antenna are,

i.   A coplanar wave guide (CPW) to coplanar strip line (CPS) transition (Figure 1a)

ii.   Tapered slot antenna with elliptical tapering (Figure 1b) and

iii.   A rectangular loop slot antenna (Figure 1c).

In this design each of these antenna elements were effectively integrated to form a dual port antenna with ultra wideband characteristics in first port and narrow band performance in the second port. The side and top view of the developed antenna in uniplanar configuration is shown in Figure 1d
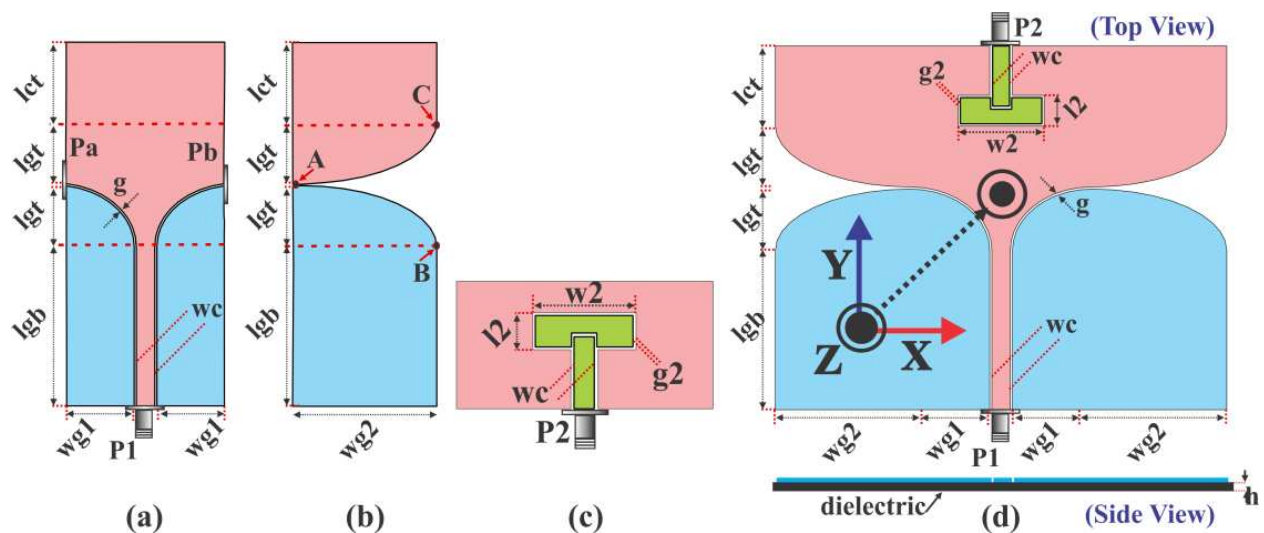

Figure 1. Geometry of the Proposed Antenna. (a) CPW to CPS transition (b) Tapered slot antenna (c) rectangular ring slot antenna (d) integrated antenna.

Design:

CPW to CPS Transition: The design is initiated by designing a coplanar waveguide with characteristic impedance 50Ω on Rogers™ TMM6 thermoset microwave laminate with dielectric permittivity (ε_r) 6, loss tangent 0.0037 and thickness (h) 0.762mm using conventional design procedure [7].The open end of the coplanar waveguide is extended with a smooth curvature to form a CPW to coplanar stripline (CPS) transition [24], which is specified by geometrical parameters lgt, wg1 and g as shown in Figure 1a. In order to maintain geometrical symmetry lgt and wg1 are maintained constant on both sides of the transmission line resulting two striplines terminated at port –Pa and port-Pb. The parameters were optimized for wide impedance bandwidth while maintaining the compact size.

Tapered Slot antenna: An elliptically tapered slot antenna characterized by two identical ellipses with X and Y radius of wg2 and lgt, respectively is shown in Figure 1b. The tapering is optimized for wideband operation specified by FCC [1], while maintaining the initial ta-

pered slot width as 'g'. The length of curvaure AB and AC are defined [25] as ¼thof the perimeter formed by the ellipse (1),

$$AB = AC = \frac{\pi}{2} \sqrt{\frac{(\lg t^2 + wg2^2}{2}}$$

(1)

Rectangular loop slot antenna: The rectangular loop slot antenna inspired from [26], with geometrical parameters l2, w2, g1 and g2 is shown in Figure 1c. The antenna is fed with an inset open circuited single layer CPW stub for good impedance matching and radiation characteristics.

The Integrated Antenna: At the first stage of integration, the elliptically tapered slot antenna is integrated to the ports Pa and Pb of CPW to CPS transition, resulting uni-planar UWB antenna configuration. The antenna parameters wg2 and lgt were fine tuned to fix the lower cut-off frequency to facilitate wide impedance bandwidth covering the FCC specified spectrum from 3.1GHz to 10.6GHz. In the second stage, the narrow band antenna with CPW feed is embedded at the space between two tapered slots, without affecting the performance of the UWB antenna. The geometrcial parameters of the antenna were optmized using commercial tool CST Microwave Studio® (CST MWS) based on finite integration technique (FIT). The optimum parameters are listed in Table 1 which are a trade off between wide impedance bandwidth, small foot print and improved isolation.

Parameters	Value, mm	Parameters	Value, mm	Parameters	Value, mm
wc	3	**lgt**	10	**l2**	5
wg1	15	**lct**	12.9	**g2**	0.5
wg2	22	**g**	0.35	**g1**	0.25
lgb	25.8	**w2**	14	**h**	0.762

Table 1. Geometrical parameters of the integrated antenna shown in Figure 1

2.2. Simulation with experimental validation

After optimizing the integrated antenna, a prototype is fabricated using LPKF® circuit board plotter. The entire fabrication process is relatively simple and can also be performed using conventional low cost PCB processing technology such as photolithography. In addition, the single layer design eliminates the requirement of alignment holes. Therefore this design facilitates accurate, efficient and cost effective fabrication. The fabricated prototype with a mechanical calibration standard is shown in Figure 2a for comparison. A perspective view of the wide-narrowband antenna mounted for measurement in the anechoic chamber is provides in Figure 2b.
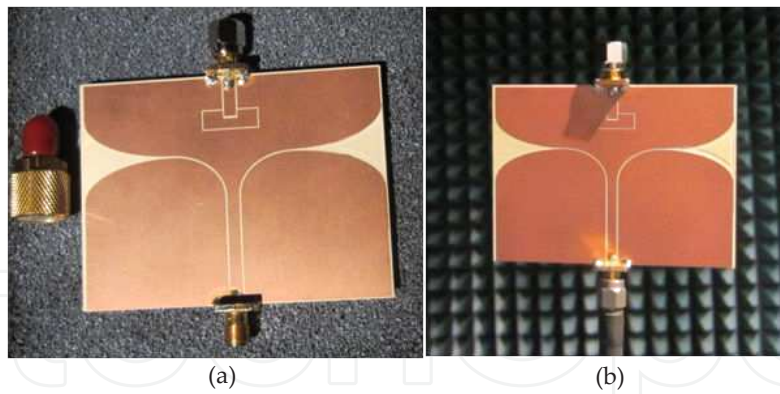
(a)   (b)

Figure 2. Photograph of the fabricated prototype (a) front view (b) perspective view

Measurement of both frequency and time domain characteristics are essential to evaluate the performance of an UWB antenna. In frequency domain the S-parameters, gain, efficiency, radiation pattern and polarization are measured and analysed in section 2.2.1. In time domain, the antenna performance is evaluated using very short pulses. The group delay, antenna transfer function, impulse response and fidelity were analysed and discussed in section 2.2.2

2.2.1. Frequency domain characteristics

The measured reflecton and transmission coefficients of the antenna along with the simulation results are plotted in Figure 3.
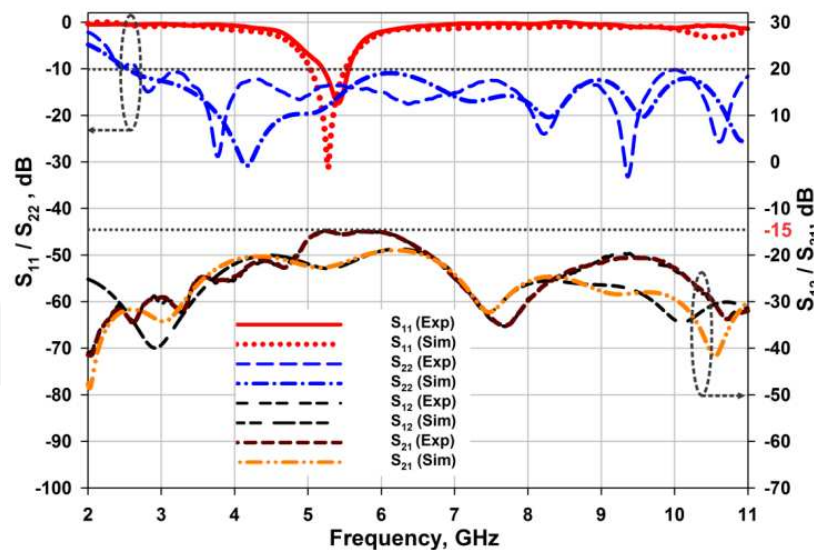

Figure 3. Simulated and measured S parameters of the Wide-Narrowband Antenna.

It is found that the UWB antenna excited through port-P1 provides a 2:1 VSWR bandwidth from 2.6GHz to 11GHz, meanwhile, the narrowband (NB) antenna excited through port-P2 provides 2:1 VSWR bandwidth from 5 GHz to 5.5 GHz. Thus the integrated antenna meets

the VSWR bandwidth requirement for the FCC specified UWB band and for the WLAN spectrum. The trasmission coefficients in Figure 3 shows that, the inter-port isolation is better than 15dB which is a reasonable value to eliminate the cross talk between the antennas. The simulated and measured s-parameters are in reasonable agreement. However, there is a slight discrepancy between the theorectical and experimental results. This is mainly because of the approximation of boundary conditions of computational domain. In addition, as explained in [27], RF cables from the vector network analyzer slightly influences the measurement of small antennas.

The isolation mechanism and polarization of the electromagnetic radiation is investigated through simulated surface current analysis. The magnitude and vector plot of surface current density at 5.2 GHz is illustrated in Figure 4.
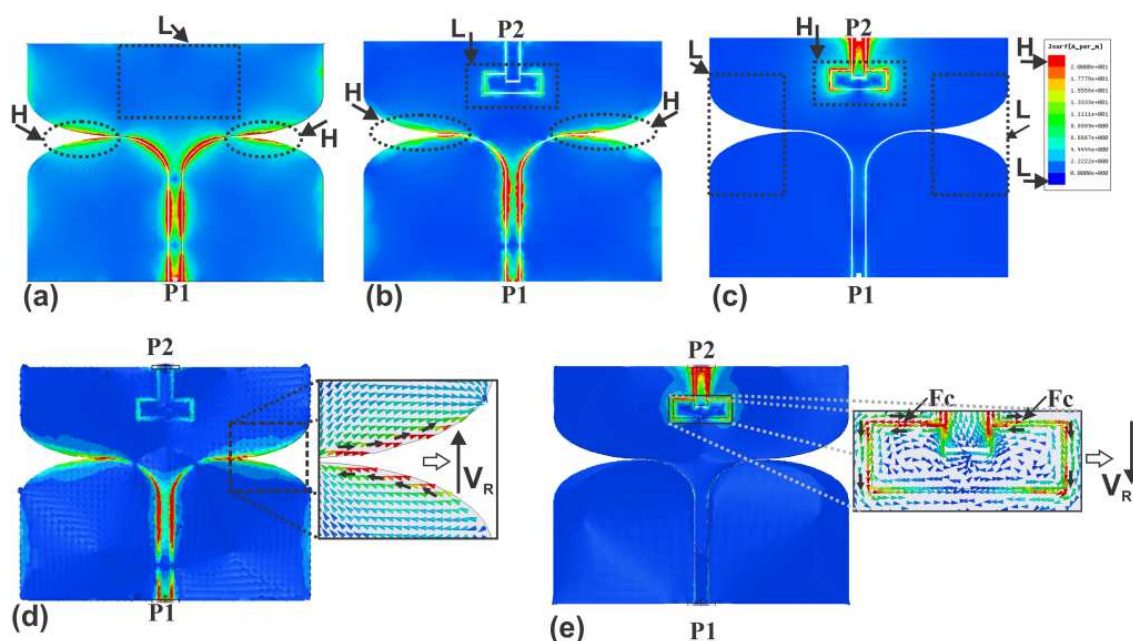

Figure 4. Simulated surface current distribution at 5.2GHz. (a) Magnitude of Jsurf of UWB antenna without integrating NB antenna (b) Magnitude of Jsurf with P1-excited, P2=50Ω (c) Magnitude of Jsurf with P2-excited, P1=50Ω (d) Vector of Jsurf with P1-excited, P2=50Ω (e) Vector of Jsurf with P2-excited, P1=50Ω

It is evident from Figure 4a that, the tapered surface regions on both sides of the integrated antenna contributes for the radiation. Meanwhile, the current excited at the top region between two tapered slot antennas, indicated by the rectangular dashed box, is almost nil. This region is effectively utilized to integrated the ring slot antenna for narrow band operation. In Figure 4b, the surface currents in the integrated configuration is provided, which shows that the current coupling from UWBA to the NBA and vice versa(figure 4c) is very low. This results in an efficient integration with good inter-port isolation. The vector analysis of surface current in the integrated antenna is shown in Figures 4 (d-e). It is clear from the plot that the dominant radiating current vector at both the tapering is vertical in direction. This shows that the polarization of the radiated electromagnetic wave from the ultra wideband antenna is vertically polarized. Similarly, the resultant current vector at the vertical slot

edges of NBA are vertical in direction and in turn results in vertical polarization. However, it is worth to note that, while estimating the composite current vector, the surface regions where equal and opposite current vectors exists, indicated by Fc, are not taken into account.
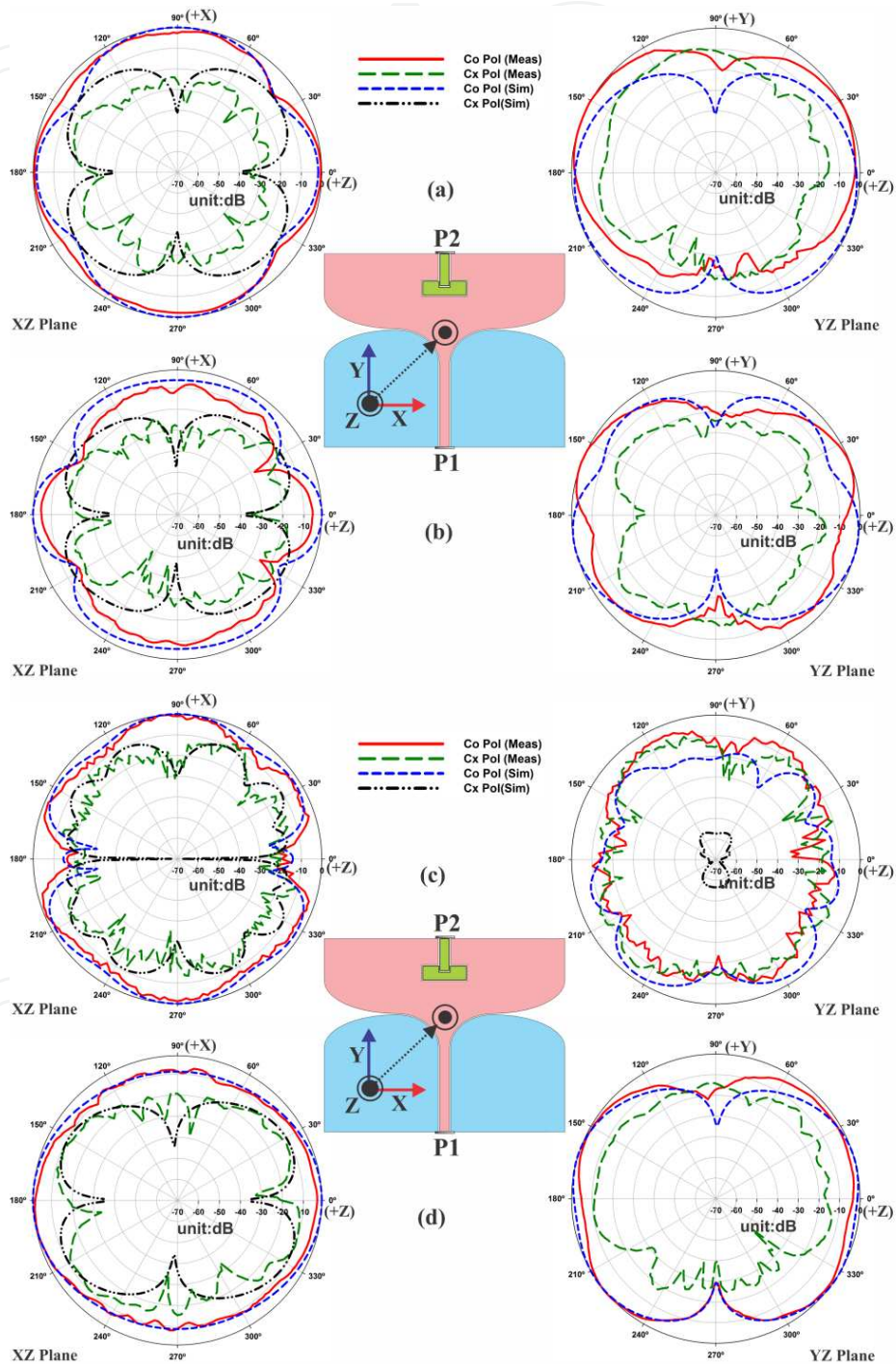

Figure 5. Measured and simulated radiation patterns (a) 3.5 GHz [P1] and (b) 5.2GHz [P1] (c) 10.5 GHz [P1] and (d) 5.2GHz [P2]

The simulated and measured radiation pattern of both the UWB and NB are presented in Figures 5(a-d). These radiation patterns were measured independently, that is, port-P2 is loaded with 50Ω termination while exciting port-P1 and vice versa. It is clear from the pattern that the UWB antenna is directional towards 0º and 180º because of the two tapered slot antennas radiating to the corresponding directions. This indicates that, the UWB and NB antenna has beam maxima at ±X and ±Z directions respectively, which are not highly attractive for applications which utilize the simultaneous utilization of both antennas.

However, the radiation patterns are suitable for cognitive radio applications such as IEEE 802.11 wireless rural area networks (WRAN) in which the spectrum sensing take plane during the interval between intra-frame and inter-frame, when the transceiver is switched off [28]. It is also visible from the radiation pattern that, at higher frequencies, the polarization purity is degraded due to the finite ground plane effect. A good agreement between simulated and measured radiation patterns are observed except for the cross polar patterns in the YZ plane. This is mainly because of the spurious reflections from the SMA connectors and cables that are not incorporated in the computational simulation. In conclusion, the patterns are similar to those observed for antennas used in cognitive radio systems [10, 22] and in wireless system terminals [29]. It is worth to note that, these patterns are also suitable for applications in indoor wireless communication systems including ad-hoc networks, where cross polar performance is not a high priority requirement and channels are dominated by rich Rayleigh fading [30]
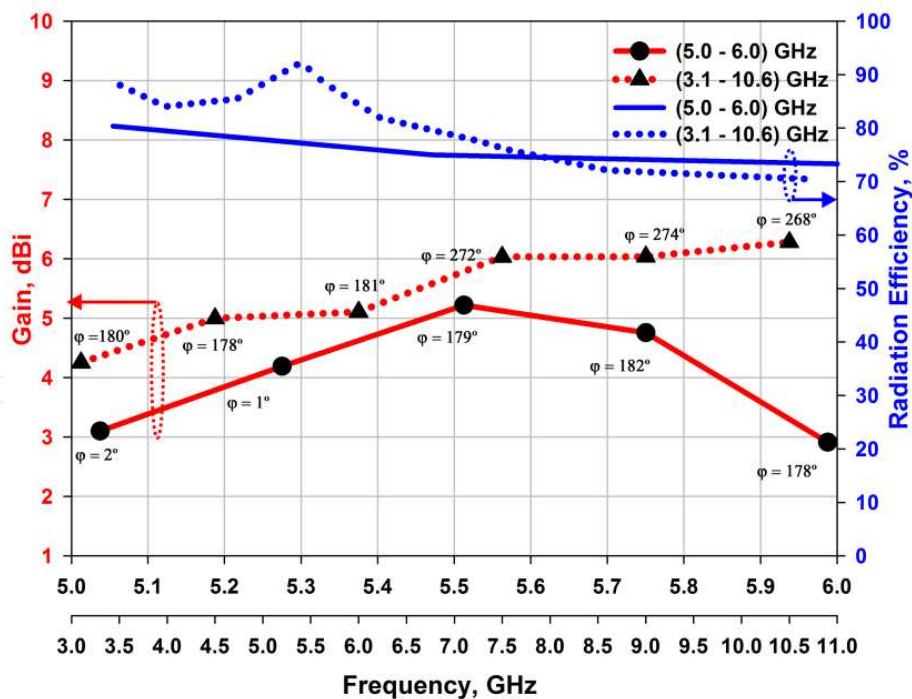

Figure 6. Separately measured gain and efficiency of UWB (port 1) and NB (port 2) antenna.

The gain of UWB and NB antenna are measured independently in the XZ-plane using the gain comparison method and shown in Figure 6. In the graph 'φ' denotes the direction of

radiation corresponding to the peak gain. It is clear from the measurement results that, the gain variations are within 2.2dBi and 2.4 dBi in the ultra wide band and narrow band spectrum of the integrated antenna, respectively. The radiation efficiency is also measured using wheeler cap method [31]and incorporated in Figure 6. It is found that the average efficiency of 81% and 75% are observed for UWB antenna and NB antenna, respectively.

2.2.2. Time domain characteristics

As depicted in the introduction, the UWB antenna need to possess high level of pulse handling capabilities in order to handle high frequency impulses. In this section the time domain characteristics including group delay, antenna transfer function, implulse response and fidelity factor were measured and discussed.

In order to measure the group delay of the UWB antenna, two identical antenna prototypes were made. As illustrated in the inset of Figure 7, these two identical antennas were kept in in the anechoic chamber at far field(R=1m) with two orientations; face-to-face and side-by-side. The time domain measurement capability of the vector network analyser is utilized for this measurement. Prior to the measurement, a full two port calibration is performed to eliminate the effects of cables and connectors. The measurement is performed by exciting the identical antennas through port-P1 while port-P2 is terminated with a broadband 50Ω termination. It is clear from Figure 7 that, the group delay remains constant with variations less than a nanosecond for both orientations.
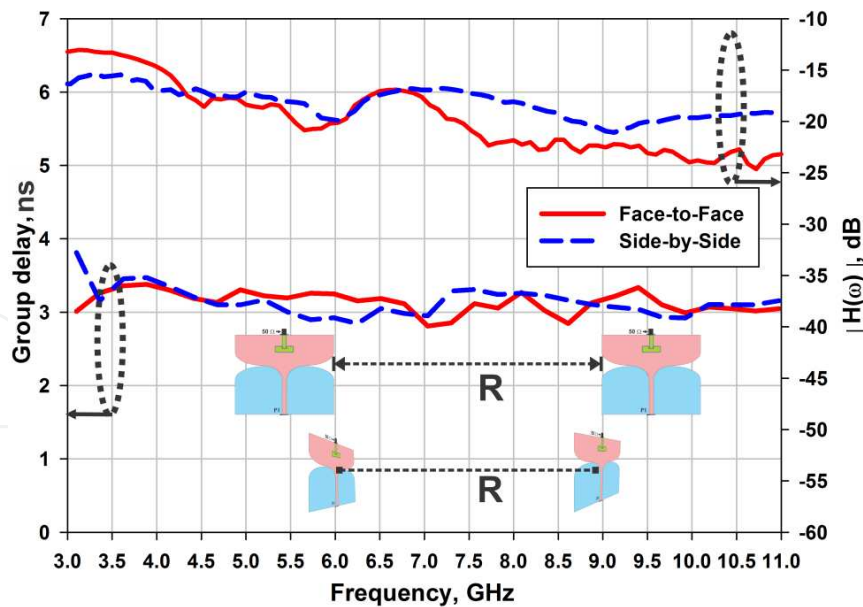

Figure 7. Measured group delay and normalized antenna transfer function in two different orientations of the UWB antenna (R = 1m)

The antenna transfer function of the antenna is also calculated using (2) and incorporated in Figure 7.

$$H(\omega) = \sqrt{\frac{2\pi R c S_{21}(\omega)e^{j\omega R/c}}{j\omega}} \qquad (2)$$

where c is the velocity of light in free space and R is the distance between two antennas [25].

The antenna transfer function remains fairly stable throughout the UWB spectrum with variations less than 10dB except for the lower end of the spectrum in the face-to-face orientation.

The transient response of the antenna is evaluated using fourth derivative of the Gaussian pulse defined by (3)

$$V_{in}(t) = A\left(3 - 6\left(\frac{4\pi}{T^2}\right)t^2 + \left(\frac{4\pi}{T^2}\right)t^4\right)e^{-2\pi\left(\frac{t}{T}\right)^2} V\left|m\right. \qquad (3)$$

The impulse response of the wideband antenna is obtained by convoluting the fourth derivative of (3) with the inverse Fourier transform of antenna transfer function (2). The spectrum of this pulse fully covers the FCC band and comply with the emission standards specified when the amplitude constant A = 1.6 and pulse duration parameter T = 67ps. [32]

The input pulse and the output pulses at face-to-face orientation and side-by-side orientation are shown in Figure 8. It is evident from the plot that the UWB antenna retains the information contained in the impulse with minimum distortion.
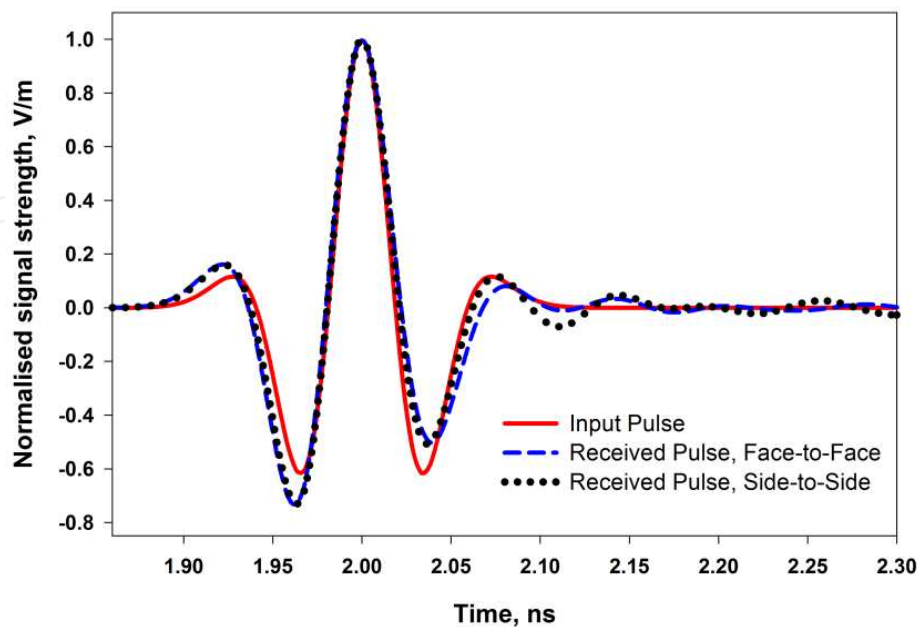

Figure 8. Input and radiated pulses of the proposed antenna.

Fidelity factor, F is an effective parameter to analyze the distortion between two pulses [33], which is defined as,

$$F = \frac{\int_{-\infty}^{\infty} S_t(t) S_r(t-\tau) d_t}{\sqrt{\int_{\alpha}^{\alpha} |S_t(t)|^2 dt \int_{\alpha}^{\alpha} |S_r(t-\tau)|^2 dt}} \tag{4}$$

where τ is the delay between the input pulse St (t) and the output pulse Sr (t). The fidelity factor of the wideband antenna is also evaluated and presented in Table 2. The fidelity factor remains greater than 0.85 which shows that, the antenna imposes negligible effects on the radiated pulses.

Orientation	Fidelity Factor,F
Face-to-Face	0.86
Side – to –Side	0.88

Table 2. Fidelity Factor of the wide band antenna

2.3. Parametric analysis

A parametric analysis of the key antenna prameters which influence the lower cut-off frequency of the UWB antenna and the resonant frequency of the NB antenna is studied in this section. This will help the antenna engineers to pay more attention to those parameters during the design, optimizaton and prototyping.
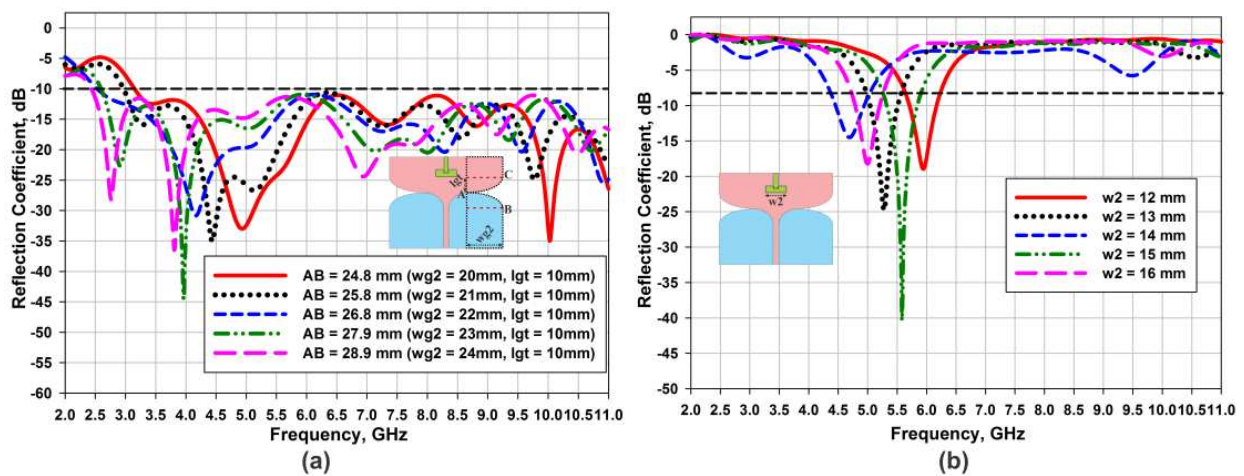

Figure 9. Influence of key antenna parameters on reflection coefficient (a) Tapering aprature, AB (b) loop width, w2

The variation of relfection coefficient with tapering aprature AB is the most sensitive parameter which determins the lower cut-off frequency of the UWB antenna. Figure 9a shows the

variation of reflection coefficient with wg2 (and in turn AB). It is clear from the plot that the lower resonance shifts drastically for small variations of wg2. As wg2 increases from 20mm to 24mm the lower cut-off frequency of the UWB antenna moves from 3.2GHz to 2.4 GHz. It is also worth to note that the impedance matching throughout the wide band remains within the FCC specifications when the tapering aprature varies from 24.8mm to 28.9mm. In narrow band antenna, the variation of resonant frequency with the loop width, w2 is depicted in Figure 9(b). It is found that when the loop width varies from 12mm to 16mm the resonant frequency of the narrow band antenna drifts from 6GHz to 4.6GHz.

2.4. Conclusion

An integrated dual port antenna with good inter-port isolation in uniplanar configuration for congnitive radio systems is presented in this section. The space between two tapered slot antennas which forms the ultra wideband antenna, is effectively utilized to integrate a narrow band sqare loop slot antenna. The measurement results indicate that, the UWB and NB antenna provides a 2:1 VSWR bandwidth from 2.7 GHz to 11 GHz and 5 GHz to 5.5GHz, respectively. The antenna also provides inter-port isolation better than 15 dB throught the resonant band. Measured readiaton pattern reveals that the wide-band antenna can fulfill the needs of spectrum searching task, and the narrow-band antenna can be used for trasmission in cognitive radio systems. The time domain characteristics of the UWB antenna in the integrated configuration is also studied and the results reveals that it facilitate transmission and reception of pulses with minimum distortion. Therefore, the antenna can also be a good candidate for future applications, such as medical imaging / weapon detection systems, which are connected to the host system through high speed WLAN link.

3. Ultra-wideband slot antenna for polarization diversity applications

In this section an Ultra wideband Antenna for polarization diversity application is presented. The development, analysis and characterization of this dual port antenna is discussed in detail. Both frequency and time domain analysis of the fabricated prototype reaveals that, this antenna is an attractive element in future wireless communication systems where the challenges such as multipatch fading is a major concern.

3.1. Antenna geometry and design

The proposed antenna is inspired from the design proposed in [34], where wideband characteristics is obtained by exciting a compact annulus ground plane with a circular patch. In this work, a polarization diversity antenna is devoloped by feeding an annulus ground plane with dual orthogonal ports. This feeding mechanism is on of the effective technique for diversity antennas [14, 17].
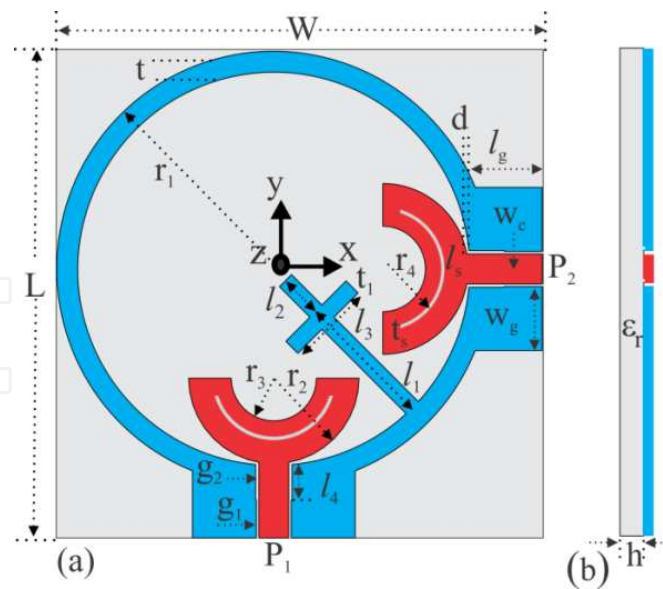
Figure 10. Geometry of the proposed antenna (a) Top view, (b) Side view

The proposed antenna geometry in cartesian coordinate system are shown in Figure 10. The basic antenna structure consists of an annulus slot and two orthogonal, identical CPW signal strips at same distance from the annulus center. Compared to dual polarized UWB slot antennas recently reported in [14, 17], the ground plane of the proposed antenna is modified as an annulus slot with radius r1 and thickness t, which creatively reduces the antenna footprint. The CPW feedline is exciting two U-shaped elements with geometrical parameter r2, r3. In addition to the the broad impedance bandwidth of this unique design, an impedance transformer with length l4 and gap g2 is also incorporated in the CPW line for further bandwidth enhancement. Since, inter-port isolation is one of the highly desirable characteristics of a diversity antenna, a cross shaped strip with dimensions l1, l2 and l3 is embedded diagonally in the antenna. In order to avoid interferences with the overlaping unlicensed bands in the UWB spectrum, an arc shaped slot resonator with specifications r4,ts and ls is also integrated in the antenna. This slot resonator facilitates band notch functionality for the diversity antenna.

Design: The antenna is realized on a Rogers® RT/Duroid 6035HTC laminate with permittivity (r) 3.6, loss tangent 0.0013, and thickness (h) 1.524mm. The CPW line with characteristics impedance 50Ω is first designed using the conventional design procedure [7]. The annulus ground plane parameters (r1) and U-shaped stub dimensions(r2,r3,d) were selected [35]to cover the FCC specified UWB spectrum. In this design the radius r1 of the ground plane determines the first resonant frequency and the radius r2 ensures the impedance matching. In conclusion, the merging of several dominant resonances, which are produced by the annulus ground, the U shaped feeding structure, and the coupling between them provides a broad impedance band width [36]. In order to increase the inter port isolation a cross shaped stub [37] is then inserted at an optimum position diagonally in the ground plane. Finally the semicircular arc shaped resonators were designed [38] and integrated for notch functionality. The antenna provides desired notch in the IEEE 802.11a and HIPERLAN/2 bands, when the length of the slot resonator ls is approximately half wave length long at the center notch frequency.
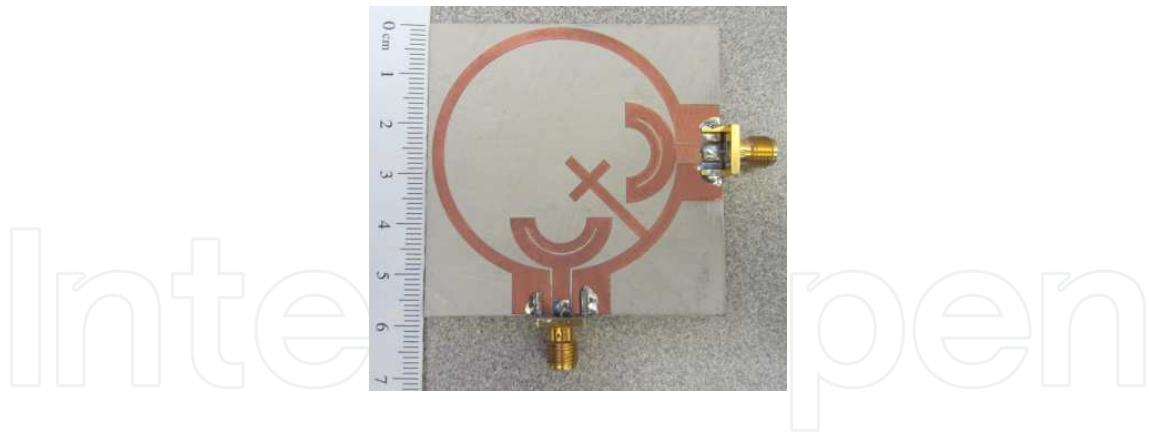
Figure 11. Photograph of the fabricated prototype

The initial analysis of the geometrical parameters and optimization of the antenna is per-formed using the FDTD based CST Microwave Studio®. The optimum parameters are listed in Table 3 which is a tradeoff between wide impedance bandwidth, better isolation, sharp notch and small foot print.

Parameters	Value, mm	Parameters	Value, mm	Parameters	Value, mm
W	57	g1	0.3	t	2.5
L	57	g2	0.4	t1	2
r1	23	d	0.2	ts	0.4
r2	10	lg	8.5	l1	16
r2	5	wg	7.5	l2	5
r4	7	wc	3.5	l3	10

Table 3. Geometrical parameters of the diversity antenna shown in Figure.10

3.2. Simulation and experimental results

After the initial design and optimization of the diversity antenna using 3D full wave electro-magnetic solver, a prototype is fabricated using LPKF milling machine. Extreme care is taken during the milling process to ensure fabrication accuracy especially at the most sensing ele-ments such as the width of the slot resonator. The fabricated prototype is shown in Figure 11. The measurement results in frequency and time domain are discussed in the following sections.

3.2.1. Frequency domain

The measured and simulated S-parameters of the proposed dual polarized antenna at port-1 (P_1) and port-2 (P_2) are presented in Figure 12. Due to geometrical symmetry the simulated results for both ports are identical. The slight difference in the measured S_{11} and S_{22} is owing to the fabrication inaccuracies. The antenna displays a 2:1 VSWR bandwidth from 2.80 GHz to 11GHz with an inter-port isolation better than 15dB except at the lower and higher fre-

quency end. It also provides a notch band with high band rejection from 4.99 to 6.25GHz. The small differences in the measured and simulated results are due to the approximate boundary conditions in the computational domain. Moreover, RF cable from the vector network analyzer slightly affects the measurements of small antennas [27]
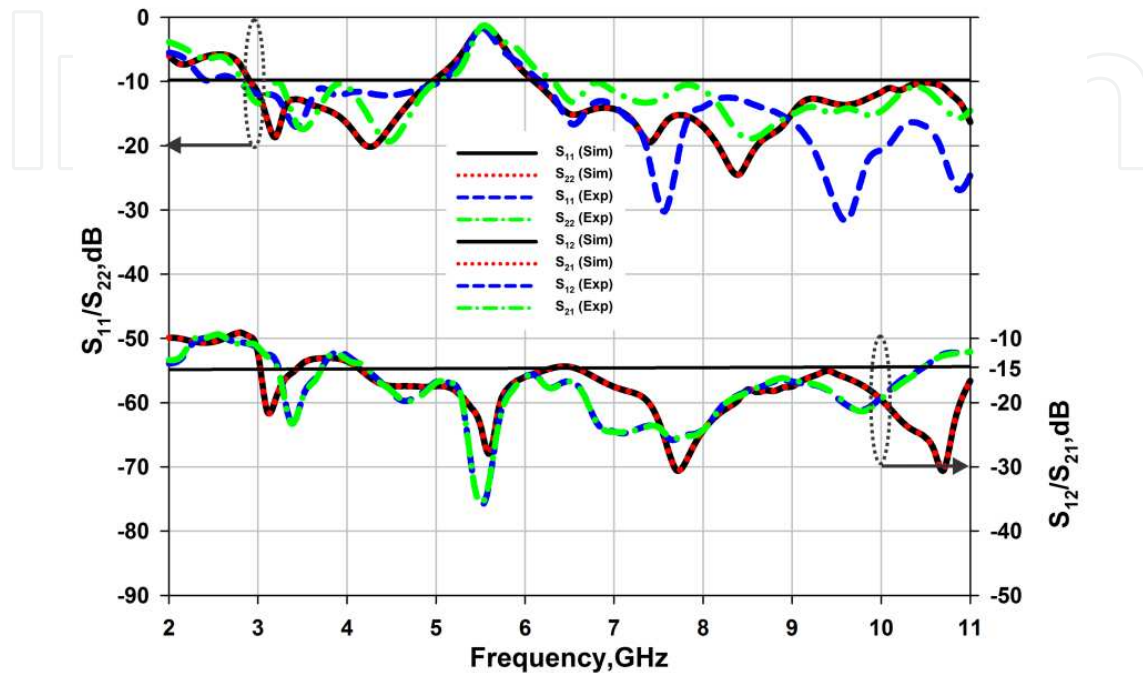

Figure 12. Simulated and Measured S-parameters of the diversity antenna.

The transmission coefficient shown in Figure 13(a) provides the influence of cross shaped stub throughout the resonant band. It is observed that, the isolation is improved by inserting the stub diagonally between the U-shaped elements. In addition the cross stub improves the impedance matching at the lower end of the spectrum.

The magnitude of surface current density at 3.5GHz and 8.5 GHz are illustrated in Figure 13(b-e) which aid better understanding about the isolation performance of the antenna. It is evident from the results that, when P1 is excited without the isolation strip, the current from P1 has a tendency to couple to P2 through the common ground plane. However the integration of the isolation strip drastically reduces the current on the ground plane around P2 (vice-versa when P2 is excited) with a strong current excitation on the strip. This results in better inter-port isolation and thereby significantly improves the diversity performance. It is also worth to note that the isolation strip has negligible influence over the surface current on the antenna elements connected through P1 at both lower and higher end of the UWB spectrum.

The far-field (2D) radiation pattern of the proposed antenna is also measured and compared with the simulation results at three different frequencies in the UWB band. The patterns are measured in a fully automated anechoic chamber, which is connected to Agilent® E8362b Performance Network Analyzer. A standard horn antenna is connected to the first port of the PNA while the second port is connected to the antenna under test. The radiation pat-

terns in the XZ and YZ planes at 3.1 GHz, 7.5 GHz and 10.5 GHz seperatly measured for both ports in orthogonal planes are illustrated in Figure 14. Nearly omnidirectional patterns are observed in the lower frequency region of the UWB spectrum meanwhile slight distortions exists at the higher frequency region. This is partially due to the effect of connecters and cables [39, 40]and magnetic current variations along the circumference of the slot [14]. It is also worth to note that the patterns at P1 and P2 are almost similar with a 90º rotation, which in turn confirms dual polarization. In general, the patters are similar to those observed for diversity applications [14] and in wireless system terminals [29]
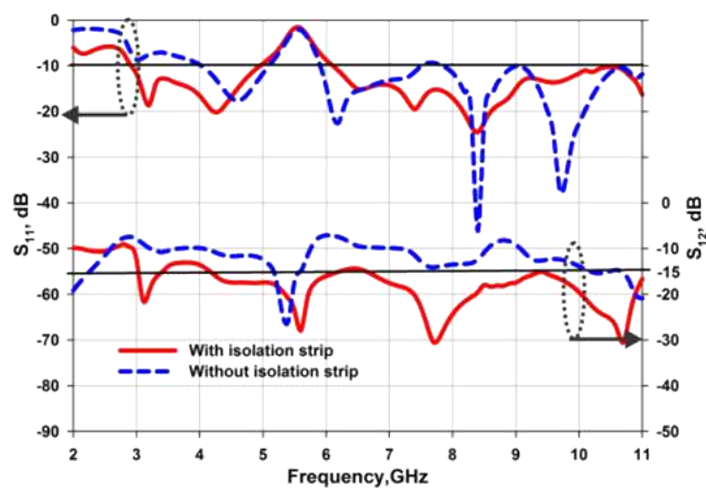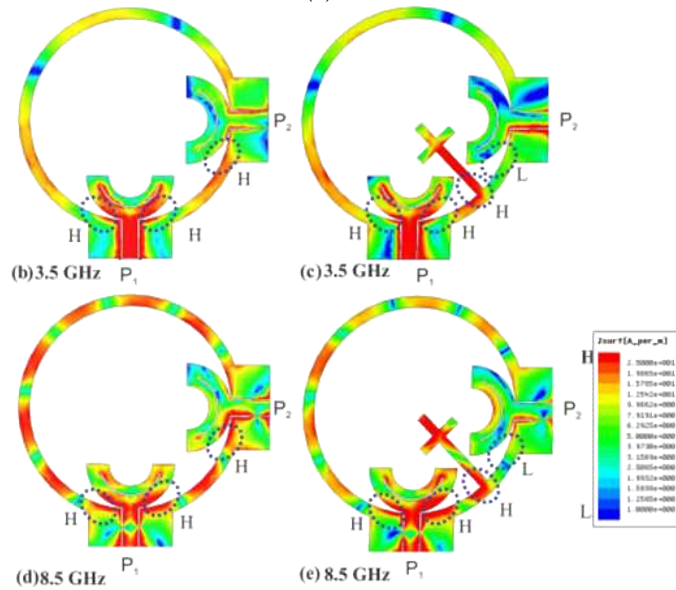
Figure 13. a) Simulated transmission coefficient, Magnitude of Jsurf (b) at 3.5GHzwithout isolation strip (c) at 3.5GHz with isolation strip (d) at 8.5GHzwithout isolation strip (e) at 8.5 GHz with isolation strip
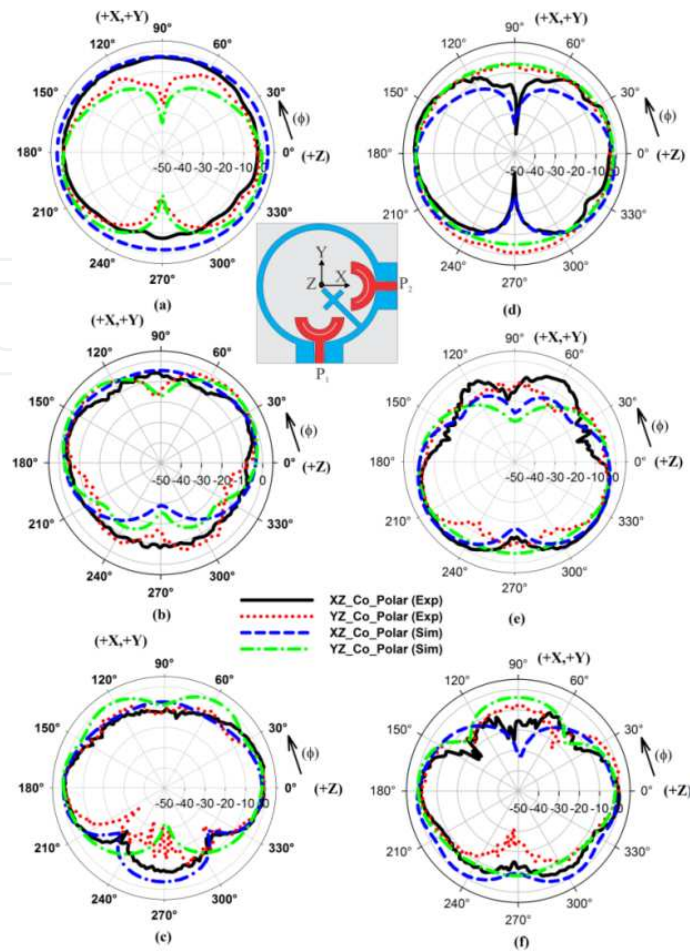
Figure 14. Measured and simulated radiation patterns (a) 3.5 GHz [P1] and (b) 7.5GHz [P1] (c) 10.5 GHz [P1] (d) 3.5 GHz [P2] and (e) 7.5GHz [P2] and (f) 10.5 GHz [P2]

In a diversity system the envelope correlation coefficient (ECC) is an important measure of diversity performance. ECC with a value of greater than 0.5 can typically degrade the diversity performance. The envelope correction coefficient of the proposed antenna is also calculated from the simulated and measured S-parameters as described in [41] using (5) and shown in Figure 15.

$$\rho_c = \frac{\left| S^*_{11} S_{22} + S^*_{21} S_{22} \right|^2}{\left(1 - \left[|S_{11}|^2 + |S_{21}|^2 \right]\right)\left(1 - \left[|S_{22}|^2 + |S_{12}|^2 \right]\right)} \tag{5}$$

It is evident from Figure 15 that, the proposed antenna has a very low value of ECC throughout the operating band which clarifies that the antenna is a good candidate for modern wireless communication systems employing polarization diversity.
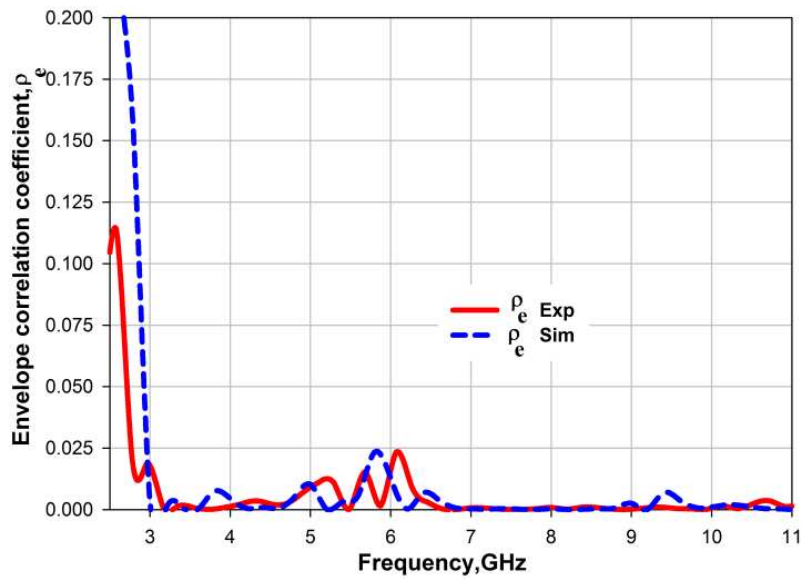
Figure 15. Measured and simulated envelope correlation coefficients from S parameters

The gain of the antenna for both ports are measured independently (when P1 is excited, P2 is terminated with 50Ω load and vice-versa) using gain comparison method. In this the gain is measured in both the planes of the radiation pattern and the peak gain is selected from either plane which gives the larger value. It is clear from the Figure 16 that, the antenna has moderate gain with variations less than 2.23dBi throughout the operating band while the gain drops up to -9.3dBi in the notch frequency.
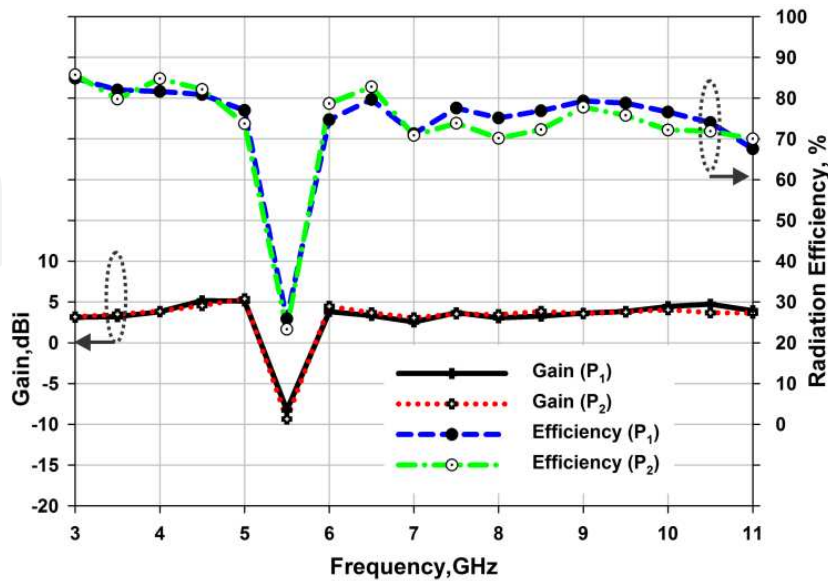

Figure 16. Measured peak gain and radiation efficiency

The efficiency of the antenna for both ports is measured using Wheeler cap method [31] and is also incorporated in Figure 16. The antenna provides efficiency better than 70% in the UWB spectrum while it drops to 25% in the notch band.

3.2.2. Time domain analysis

Advanced UWB systems are realized using an impulse-based technology in which the time domain performance are equally as important as frequency domain properties. The time domain characteristics including group delay, antenna transfer function, impulse response and fidelity are measured, analyzed and discussed in this section.

The group delay of the antenna for face to face orientation is measured using the time domain measurement facility of Anritsu Ms4647A network analyzer by exciting two identical antennas kept in the far field (when P_1 is excited P_2 is terminated with 50 Ω load and vice-versa).The antenna provides a group delay (Figure 17) which remains almost constant with variations less than 1ns except at the notch band. The antenna transfer function defined by (2) is also calculated and incorporated in Figure 17.It shows fairly flat magnitude variations for each port of the antenna, which is less than 10dB throughout the band. The impulse response of the antenna is evaluated by convoluting the modulated Gaussian monocycle defined in (3) with h(t), the inverse Fourier transform of antenna transfer function. The spectrum of this impulse fully covers the FCC band and comply with the emission standards specified when, the amplitude constant A = 1.6 and pulse duration parameter T = 67ps. The input and output waveforms for both ports are shown in Figure 18. It can be seen that the radiated pulse through two ports of the proposed antenna retain the information with minimum dispersion.
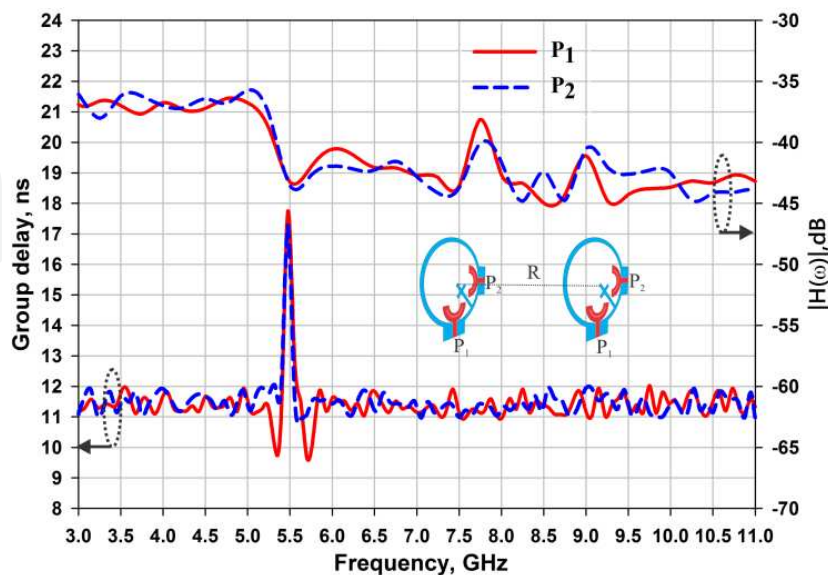

Figure 17. Measured group delay and antenna transfer function between identical antennas
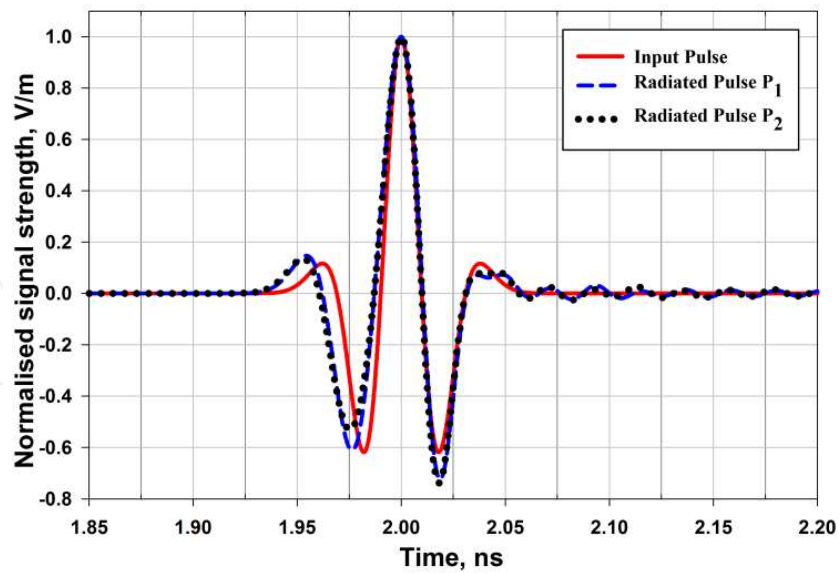
Figure 18. Input and output impulses through P_1 and P_2 of the antenna

The cross correlation between the source pulse St (t) and the radiated pulse Sr(t) is then evaluated by the fidelity factor, F using (4). As shown in Table 4, high value of Fidelity reveals that the antenna imposes negligible effects on the transmitted pulses [42].

Orientation	Fidelity Factor
P1	0.88
P2	0.85

Table 4. Fidelity Factor of the proposed antenna for both ports.

3.3. Parametric analysis

In order to provide more information to the antenna engineers during the design and optimization process, a parametric analysis of important antenna parameters which influence the lower cutoff frequency (r_1) and notch band (*l*s) are conducted and presented.

Figure 19a shows that the first resonant frequency of the antenna drifts down when the ground radius r1 is increased from 22 to 25 mm. This clarifies the initial assumption that, the first resonance frequency is determined by the radius r1. It is also clear that the ground strip length has a slight influence on the isolation characteristics. An optimum value r1=23mm is selected for required performance. The tuning of notch band with slot length ls is shown through the parametric analysis in Figure 19b. As the ls varies from 16mm to 20mm, the peak notch frequency shifts from 6.1 GHz to 5GHz. These parameters are very sensitive to the overall performance of the antenna and therefore it is required to provide extreme care during the fabrication process.
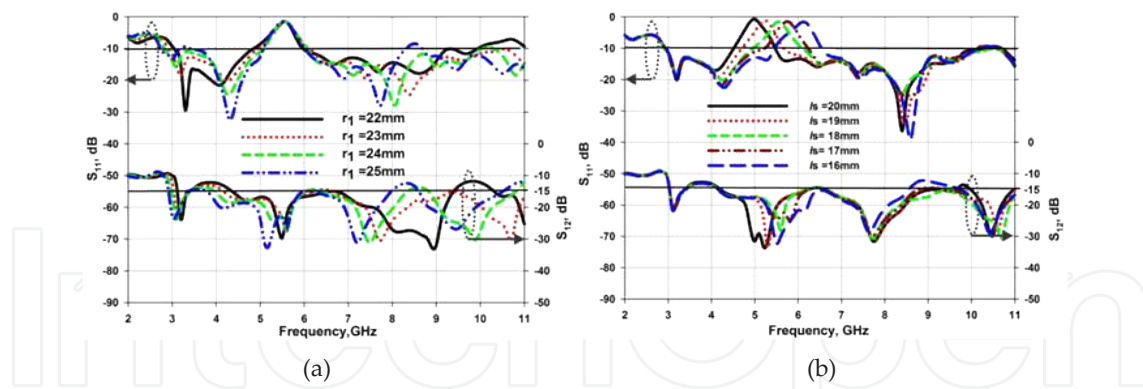
Figure 19. Effect of major antenna parameters on antenna characteristics (a) r1 (b) ls

3.4. Conclusions

A compact uniplanar dual polarized UWB antenna with notch functionality is developed for diversity applications. The antenna features a 2:1 VSWR band from 2.8-11 GHz while showing the rejection performance in the frequency band 4.99-6.25 GHz along with a reasonable isolation better than 15dB. The measured radiation pattern and the envelop correlation coefficient indicate that the antenna provides good polarization diversity performance. Time domain analysis of the antenna shows faithful reproduction of the transmitted pulse even with a notch band.

Acknowledgements

Author details

Gijo Augustin , Bybi P. Chacko and Tayeb A. Denidni

National Institute of Scientific Research (INRS), Montreal QC, Canada

References

[1] FCC, "First Report and Order: Revision of Part 15 of the Commissions Rules Regarding Ultra-Wideband Transmission Systems," ET Docket 98-153, Apr. 2002.

[2] Chung, K., Kim, J., & Choi, J. "Wideband microstrip-fed monopole antenna having frequency band-notch function," Microwave and Wireless Components Letters, IEEE, vol. 15, no.11 pp. 766-768, (2005). .

[3] K. S. Ryu and A. A. Kishk, "UWB antenna with single or dual band-notches for lower WLAN band and upper WLAN band," Antennas and Propagation, IEEE Transactions on, vol. 57,no.12 pp. 3942-3950, 2009.

[4] A. Kishk, K. F. Lee, C. E. Smith, and D. Kajfez, "Microstrip Line and CPW FED Ultra Wideband Slot Antennas with U-Shaped Tuning Stub and Reflector," Progr. Electromagn. Res., vol. 56,pp. 163-182, 2006.

[5] X. H. Wu and A. A. Kishk, "Study of an ultrawideband omnidirectional rolled monopole antenna with trapezoidal cuts," Antennas and Propagation, IEEE Transactions on, vol. 56,no.1 pp. 259-263, 2008.

[6] S. L. S. Yang, A. A. Kishk, and K. F. Lee, "Wideband circularly polarized antenna with L-shaped slot," Antennas and Propagation, IEEE Transactions on, vol. 56,no.6 pp. 1780-1783, 2008.

[7] Coplanar waveguide circuits, components, and systems. Wiley-interscience, 2007 2001.

[8] Federal Communications Commission, "Spectrum Policy Task Force," Rep.ET Docket, Nov. (2002). (02-135), 02-135.

[9] P. J. Gibson, "The Vivaldi Aerial," in Microwave Conference, 1979. 9th European, 1979, pp. 101-105.

[10] E. Ebrahimi, J. R. Kelly, and P. S. Hall, "Integrated Wide-Narrowband Antenna for Multi-Standard Radio," IEEE Trans. Antennas Propag., vol. 59,no.7 pp. 2628-2635, Jul 2011.

[11] M. Sonkki, E. Antonino-Daviu, M. Ferrando-Bataller, and E. T. Salonen, "Planar Wideband Polarization Diversity Antenna for Mobile Terminals," Antennas and Wireless Propagation Letters, IEEE, no.99 pp. 1-1, 2011.

[12] R. G. Vaughan and J. B. Andersen, "Antenna diversity in mobile communications," Vehicular Technology, IEEE Transactions on, vol. 36,no.4 pp. 149-172, 1987.

[13] W. K. Toh, Z. N. Chen, X. Qing, and T. See, "A planar UWB diversity antenna," Antennas and Propagation, IEEE Transactions on, vol. 57,no.11 pp. 3467-3473, 2009.

[14] M. Gallo, E. Antonino-Daviu, M. Ferrando, M. Bozzetti, J. Molina-Garcia-Pardo, and L. Juan-Llacer, "A Broadband Pattern Diversity Annular Slot Antenna," Antennas and Propagation, IEEE Transactions on, no.99 pp. 1-1, 2011.

[15] C. B. Dietrich Jr, K. Dietze, J. R. Nealy, and W. L. Stutzman, "Spatial, polarization, and pattern diversity for wireless handheld terminals," Antennas and Propagation, IEEE Transactions on, vol. 49,no.9 pp. 1271-1281, 2001.

[16] Z. N. Chen and T. See, "Diversity and its applications in ultra-wideband antennas," 2009, pp. 1-4.

[17] R. Yahya and T. A. Denidni, "Design of a new dual-polarized ultra-wideband planar CPW fed antenna," 2011, pp. 1770-1772.

[18] X. Bao and M. Ammann, "Wideband Dual-Frequency Dual-Polarized Dipole-Like Antenna," Antennas and Wireless Propagation Letters, IEEE, vol. 10,pp. 831-834, 2011.

[19] G. Adamiuk, T. Zwick, and W. Wiesbeck, "Compact, dual-polarized UWB-antenna, embedded in a dielectric," Antennas and Propagation, IEEE Transactions on, vol. 58,no.2 pp. 279-286, 2010.

[20] G. Adamiuk, L. Zwirello, S. Beer, and T. Zwick, "Omnidirectional, dual-orthogonal, linearly polarized UWB Antenna," 2010, pp. 854-857.

[21] H. Yoon, Y. Yoon, H. Kim, and C. H. Lee, "Flexible ultra-wideband polarisation diversity antenna with band-notch function," Microwaves, Antennas & Propagation, IET, vol. 5,no.12 pp. 1463-1470, 2011.

[22] F. Ghanem, P. S. Hall, and J. R. Kelly, "Two port frequency reconfigurable antenna for cognitive radios," Electron. Lett., vol. 45,no.11 pp. 534-535, May 21 2009.

[23] J. R. Kelly, P. Song, P. S. Hall, and A. L. Borja, "Reconfigurable 460 MHz to 12 GHz antenna with integrated narrowband slot," Progr. Electromagn. Res.Lett., vol. 24,pp. 137-145, Sept. 2011.

[24] B. C. Wadell, "Trasmission line design handbook," Artech House, Inc., 1991.

[25] M. Gopikrishna, D. D. Krishna, C. K. Anandan, P. Mohanan, and K. Vasudevan, "Design of a Compact Semi-Elliptic Monopole Slot Antenna for UWB Systems," Antennas and Propagation, IEEE Transactions on, vol. 57,no.6 pp. 1834-1837, 2009.

[26] Carrasquillo-Rivera, R. A. R. Solis, and J. G. Colom-Ustariz, "Tunable and dual-band rectangular slot-ring antenna," in Antennas and Propagation Society International Symposium, 2004. IEEE, 2004, pp. 4308-4311 Vol.4.

[27] C. Zhi Ning, Y. Ning, G. Yong-Xin, and M. Y. W. Chia, "An investigation into measurement of handset antennas," Instrumentation and Measurement, IEEE Transactions on, vol. 54,no.3 pp. 1100-1110, 2005.

[28] P. S. Hall, P. Gardner, and A. Faraone, "Antenna Requirements for Software Defined and Cognitive Radios," Proceedings of the IEEE, vol. PP,no.99 pp. 1-9, 2012.

[29] K.L.Wong, "Planar Antennas for wireless communication," Wiley Interscience, New York, 2003.

[30] Y. J. Guo, A. Paez, R. A. Sadeghzadeh, and S. K. Barton, "A circular patch antenna for radio LAN's," Antennas and Propagation, IEEE Transactions on, vol. 45,no.1 pp. 177-178, 1997.

[31] H. G. Schantz, "Measurement of UWB antenna efficiency," in Vehicular Technology Conference, 2001. VTC 2001 Spring. IEEE VTS 53rd, 2001, pp. 1189-1191 vol.2.

[32] W. Sörgel and W. Wiesbeck, "Influence of the antennas on the ultra-wideband transmission," Eurasip journal on applied signal processing, vol. 2005,pp. 296-305, 2005.

[33] N. Telzhensky and Y. Leviatan, "Novel method of UWB antenna optimization for specified input signal forms by means of genetic algorithm," Antennas and Propagation, IEEE Transactions on, vol. 54,no.8 pp. 2216-2225, 2006.

[34] M. Chen and J. Wang, "Compact CPW-fed circular slot antenna for ultra-wideband applications," 2008, pp. 78-81.

[35] T. Denidni and M. Habib, "Broadband printed CPW-fed circular slot antenna," Electron. Lett., vol. 42,no.3 pp. 135-136, 2006.

[36] X. Qing and Z. Chen, "Compact coplanar waveguide-fed ultra-wideband monopole-like slot antenna," Microwaves, Antennas & Propagation, IET, vol. 3,no.5 pp. 889-898, 2009.

[37] Y. Cheng, W. Lu, C. Cheng, W. Cao, and Y. Li, "Printed diversity antenna with cross shape stub for ultra-wideband applications," 2008, pp. 813-816.

[38] N. Trang, D. Lee, and H. Park, "Compact printed CPW-fed monopole ultra-wideband antenna with triple subband notched characteristics," Electron. Lett., vol. 46,no. 17 pp. 1177-1179, 2010.

[39] Liang, C. C. Chiau, X. Chen, and C. G. Parini, "Study of a printed circular disc monopole antenna for UWB systems," Antennas and Propagation, IEEE Transactions on, vol. 53,no.11 pp. 3500-3504, 2005.

[40] Y. J. Cho, K. H. Kim, D. H. Choi, S. S. Lee, and S. O. Park, "A miniature UWB planar monopole antenna with 5-GHz band-rejection filter and the time-domain characteristics," Antennas and Propagation, IEEE Transactions on, vol. 54,no.5 pp. 1453-1460, 2006.

[41] S. Blanch, J. Romeu, and I. Corbella, "Exact representation of antenna system diversity performance from input parameter description," Electron. Lett., vol. 39,no.9 pp. 705-707, 2003.

[42] M. Tzyh-Ghuang and J. Shyh-Kang, "Planar miniature tapered-slot-fed annular slot antennas for ultrawide-band radios," Antennas and Propagation, IEEE Transactions on, vol. 53,no.3 pp. 1194-1202, 2005.